

Birleanu, C. and Pustan, M., 2017. Size effect on stiffness and pull-off force of thermally actuated gold cantilevers. *Romanian Journal of Technical Sciences – Applied Mechanics*, 62(2), pp.145–161.

## SIZE EFFECT ON STIFFNESS AND PULL-OFF FORCE OF THERMALLY ACTUATED GOLD CANTILEVERS

CORINA BIRLEANU, MARIUS PUSTAN

*Abstract.* This paper focuses on revealing the size effect on the mechanical behavior (*i.e.* bending stiffness, Young modulus, pull-off force) of gold cantilevers with lengths ranging from 190  $\mu\text{m}$  to 490  $\mu\text{m}$ . We investigated the temperature influence (from 20°C to 100°C) on the mechanical behavior of thermally actuated microcantilevers by using an atomic force microscope. The investigated cantilevers are fabricated from gold with a width of flexible part equal by 35  $\mu\text{m}$  and a thickness of 2  $\mu\text{m}$ . The flexible part of cantilever is suspended at 2  $\mu\text{m}$  above a silicon substrate. The beam anchor has a rectangular cross-section with the side of 110  $\mu\text{m}$  and the thickness of 4  $\mu\text{m}$ . A nonlinear variation of the bending stiffness of microcantilevers as a function of temperature is experimentally determined. The variation of the pull-off force between microcantilevers and substrate is monitored at different temperatures. Finite element analysis is used to visualize the thermal field in microcantilever and to compute the axial expansion. It was noted that the relaxation of the modulus of elasticity of microcantilevers with temperature is slightly higher. This investigation was found to be more versatile since it yielded additional information about the structure and material properties. The results obtained in the study are important in order to enhance the design of MEMS and to increase their reliability and the lifetime. Moreover, the results are extremely useful in understanding and controlling the mechanical characteristics of sensing/acting microcomponents under thermal operating conditions. The results are promising for applications in MEMS where accurate properties of the thermally actuated MEMS cantilevers are required within extended temperature range.

*Key words:* microcantilevers, size effect, stiffness, pull-off force, temperature.

### 1. INTRODUCTION

Microelectromechanical Systems (MEMS) have occurred into existence only in the last decade. Because of the large surface area to volume ratio of MEMS, surface effects such as electrostatics and wetting dominate over volume effects such as inertia or thermal mass [1, 2].

Among the different structures of MEMS devices the micro-cantilever beams are of great interest being used in a wide variety of applications due to the fact that they are developed and manufactured in a simple way and also due to well-established bases to study the behavior and performance.

---

Technical University of Cluj-Napoca, Department of Mechanical Systems Engineering, Micro and Nano Systems Laboratory, Cluj-Napoca, Romania

Ro. J. Techn. Sci. – Appl. Mechanics, Vol. 62, N° 2, P. 145–161, Bucharest, 2017

Microcantilevers have been employed for physical, chemical and biological sensing. These sensors have several advantages over the conventional analytical techniques in terms of high sensitivity, low cost, simple procedure, non-hazardous procedures and quick response [3]. Micro-cantilevers have been advantageously used for scanning probe in atomic force microscopy [4, 5], particle mass sensing [6], frequency doublers in electrical signal processing [6] and in a variety of other practical applications in automotive, aerospace and medical industries [2]. For micro cantilevers used as actuators, the thermal actuation method has some benefits over other methods.

For instance, the integration of heating elements in micro-systems is more beneficial than the piezoelectric and electrostatic, and thermal/electro-thermal actuation [6, 7] is widely used for real-world applications. There are several options for heating materials to be used and the amount of forces can be generated with lower power input [2, 8]. Moreover, due to the small length and miniature volume of the components, the constant thermal time of the part (actuator) is very short which in turn allows the micro-beam to heat/cool in a very short time period [6].

Changes in temperature and heat can bend a cantilever composed of materials with different thermal expansion coefficients by the bimetallic effect. Microcantilever based sensors can measure changes in temperature as small as  $10^{-5}$  K and can be used for photo thermal measurement. They can detect heat changes with attojoule sensitivity [3, 9]. Thus a cantilever is used as a tool to evaluate the change of stress occurring in its material, caused for example by changes in temperature. Experience shows that variations in temperature greatly affect the elastic and mechanical characteristics of materials. In engineering applications the structures that work at temperatures much different from the environment (temperatures extremely high or low) analyzes the behavior of materials according to the temperature is complex and very important. In order to increase design performance and reliability of these devices when they work under thermal operating conditions it is important to determine experimentally the mechanical and tribological characteristics of microcomponents.

Our work is based on this statement and in this paper, the experimental tests were carried out on microcantilevers of different sizes and in different temperature conditions using an atomic force microscope (AFM) in order to characterize through a mechanical and tribological point of view these components. At present we cannot say that there is an accurate database from which this information can be taken, depending on the microstructure and material used. This work brings important contributions in creating such a database and the obtained data represent a real item in the toolbox of the MEMS designer.

First section of the paper presents the cases of microcantilevers used as actuators that are characterized here by in plane moving due to thermal expansion or out of plane moving due to bending effects. In Section 2 of the paper is presented the principle effect of axial thermal expansion and also the relation

between bending stiffness and theoretical consideration about adhesion. Using the AFM in scanning mode the experimental results of axial expansions on the gold microcantilevers as a function of temperature (range between 20°C and 100°C) and different lengths (size effect) is presented in Section 3. To analyze the distribution of thermal field in cantilever and axial displacement of the free end of the cantilever subjected to a concentrated external load we used the finite element simulation. Also, Section 3 is focused on experimental investigation of the microcantilever bending stiffness and the dependence between stiffness and temperature. Withal are presented the thermal effects on the adhesion force between microcantilever and AFM tip using AFM technique in spectroscopy in point mode. In Section 4 shall be drawn several conclusions of this work.

## 2. THEORETICAL CONSIDERATIONS

### 2.1. Axial thermal expansion of a microcantilever

Almost all materials expand with temperature increase. This phenomenon is due to the asymmetric nature of interatomic interaction forces and increasing amplitude vibrations to the temperature as shown in the molecular-kinetic theory.

It is considered the cantilever shown in Fig. 1, which has a length  $l_0$  at ambient temperature. The width of the cantilever is  $w_0$ . To equilibrium the cantilever is unstressed and unstrained, and everywhere the temperature is  $T_0$ . If  $l_0$  is the length of the temperature  $T_0$ , then the length  $l$  at the temperature  $T$  can be determine from the equation below:

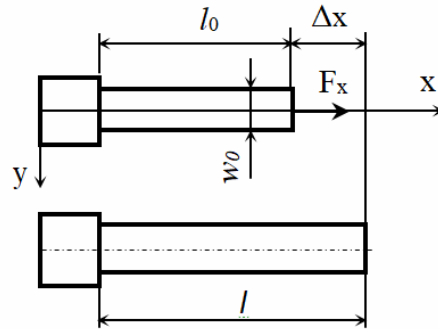


Fig. 1 – Top view of a microcantilever at the ambient temperature and after thermal expansion.

$$l = l_0 [1 + \alpha(T - T_0)] \quad (1)$$

where  $\alpha$  is the coefficient of linear thermal expansion.

In the paper we will use a constant value of the linear coefficient of thermal expansion which value is one third of the volumetric coefficient of thermal expansion [10]. The thermal expansion  $\Delta x$  can also be produced by an equivalent force that acts at the free-end of the microcantilever  $F_x$  [11]. Equation (2) gives us this force relation:

$$F_x = E \cdot S \cdot \frac{\Delta x}{l_0} = E \cdot S \cdot \alpha \cdot \Delta T, \quad (2)$$

where:  $E$  is the Young's modulus of the microcantilever material and  $S$  is the cross-sectional area.

For a thermal actuator such as a heat-actuated cantilever, its performance depends on the force that must be defeated. For example, if a load  $F$  is applied in the opposite direction of the thermal expansion, the total displacement of the free end of the cantilever will be the difference of the two opposing deformations, more precisely:

$$\Delta x = \alpha \cdot l_0 \cdot \Delta T - \frac{F \cdot l_0}{E \cdot S}. \quad (3)$$

From eq. (3) results:

$$F = E \cdot S \cdot \alpha \cdot \Delta T - \frac{E \cdot S \cdot \Delta x}{l_0} = E \cdot S \left( \alpha \cdot \Delta T - \frac{\Delta x}{l_0} \right). \quad (4)$$

## 2.2. Bending effect on a thermally actuated cantilever

The sketch of a constant rectangular cross-section microcantilever is shown in Fig. 2, it is thermally actuated and subjected to bending stress on  $x$  direction ( $\Delta z$  is the bending displacement of the microcantilever free-end). Because the dimensions of the beam,  $w_0$  and  $t_0$ , are sufficiently small compared to the length  $l_0$ , we consider the usual Euler-Bernoulli assumption that the transverse of the beam and the radius of curvature  $R$  of the bending that any plane cross section, initially perpendicular to the axis of the beam, remains plan and perpendicular to the neutral surface during bending [10].



Fig. 2 – Free-end beam. The beam bends under the action of the force in  $z$ -direction.

If we consider a microcantilever which is subject to a bending stress and also integrating a thermal effect we must consider the relaxation with temperature of the elasticity modulus [11]. We also took into consideration that the strain appears both mechanical stress and thermal expansion.

A thermoelastic solid temperature field provides an energy dissipation mechanism that allows the system to relax and in case of the investigated thermoelastic microcantilever under bending displacement the stress relaxation is determined by considering relaxation of the Young's modulus:

$$\Delta_E = \frac{E_{ad} - E_T}{E_T} = \frac{E_T \alpha^2 \Delta T}{C_p}, \quad (5)$$

whose value is known from basic thermodynamics. Here  $E_{ad}$  is the unrelaxed, or adiabatic, value of Young's modulus and  $E_T$  is its relaxed, or isothermal, value and  $C_p$  is the heat capacity per unit volume at constant pressure, or stress [10, 11]. This relaxation effect of the stress in microcantilever especially has an effect on stiffness but also on the coefficient of friction.

Whether force is applied to the free end in the direction  $z$  the stiffness of the cantilever subjected to temperature can be written as [11]:

$$k_z = \frac{E_T \cdot w_0 \cdot t_0^3 (1 + \alpha \Delta T)}{4l_0^3}, \quad (6)$$

where  $k_z$  is cantilever stiffness in  $z$  direction and  $t_0$  is the initial microcantilever thickness. And the force is:

$$F_z = \frac{E_T \cdot w_0 \cdot t_0^3 (1 + \alpha \Delta T)}{4l_0^3} \cdot \Delta z, \quad (7)$$

where  $\Delta z$  is the bending displacement of the microcantilever free-end.

Based on equation (7) it could be estimated Young's modulus versus temperature:

$$E_T = \frac{4l_0^3}{w_0 \cdot t_0^3 (1 + \alpha \Delta T)} \cdot \frac{F_z}{\Delta z} = \frac{4l_0^3}{w_0 \cdot t_0^3 (1 + \alpha \Delta T)} \cdot k_z. \quad (8)$$

### 2.3. Stiction and adhesion considerations

The stiction problem in MEMS devices can be divided into two categories depending on the situation: release-related stiction and stiction that occurs during operation (in-use stiction) [12]. As a result, adhesion and stiction can lead to catastrophic failure that deserves attention.

Once contact is made adhesion forces that occur can become stronger than the restoring elastic forces that the beams will stick to the substrate. In order to avoid in-use stiction adhesion forces should therefore be minimized, which means that the adhesion phenomenon should be known in detail up the microstructure level.

Incidental contact during operation cannot always be excluded. The applied load has an upper limit beyond which the mechanical restoring force of the microcantilever can no longer resist thereby leading to the collapse of the structure. This structural instability phenomenon is known as ‘pull-in’. Furthermore, devices are made where contact between moving parts is desirable [6, 8]. Therefore, in this case it is important to minimize adhesion forces. This can be done either by reducing the contact area or by changing the surface properties.

An important role in adhesion plays the surface roughness. From [13] was measured the root mean square average of the profile height deviations from the mean line, recorded within the evaluation length (RMS) which is approximately 0.95 nm for the 100 nm thick Au film, 2.21 nm for 300 nm thick Au film and around 2.61 nm for the 500 nm thick Au film. RMS is considered to be more sensitive than the average roughness for large deviations from the mean line/plane  $R_a$ . The surface roughness increases the magnitude of the Van der Waals forces over its value when the two surfaces are smooth [14, 15].

In this paper, as to analyze the phenomenon of adhesion depending on the temperature, we assume that the contact surfaces are perfectly flat so the actual contact area can be a large fraction of the apparent contact area between these microstructures. The mechanism of adhesion plays an important role in stiction when the mobile MEMS microstructures brought to the substrate are caused by capillary forces, hydrogen bridging, electrostatic forces and Van der Waals forces.

Mastrangelo and Hsu in [16] have shown that when the microstructure touches the substrate, the total surface energy is lowered. When the cantilever touches the substrate and the total energy of the system reaches a minimum level (during peel off phenomenon) structure will stick permanently to the substrate.

They proposed a dimensionless number, called peel number. This peel number,  $N_p$ , is the ratio of the elastic deformation energy stored in the deformed microstructure to the work of adhesion between the microstructure and the substrate. The microstructure will not join the substrate if  $N_p > 1$ , more exactly the restored elastic strain energy is greater than the work of adhesion. Furthermore, when  $N_p \leq 1$ , the deformed microstructure does not have enough energy to overcome the adhesion between the beam and the substrate [16].

The beam attaches to the substrate at distance  $l_0 - l_x$  from the anchor (Fig. 3). The elastic energy stored in the cantilever is:

$$U_m = \frac{E \cdot t_0^3 \cdot g_0^2 \cdot w_0}{2(l_0 - l_x)^3}. \quad (9)$$

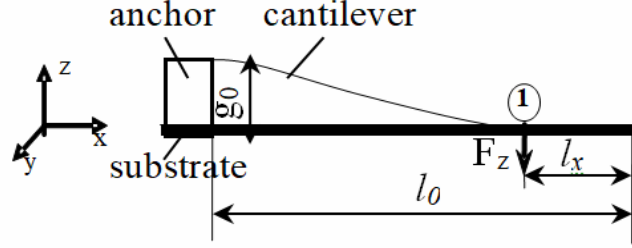


Fig. 3 – The beam attaches the substrate at distance  $x$  from the anchor ( $S$ -shape deflection).

The surface energy as a function of the attachment length  $l_x$  is:

$$U_s = C - \gamma_s \cdot l_x \cdot w_0, \quad (10)$$

where  $C$  takes into account the constant terms and  $\gamma_s$  is the adhesion energy per unit area (work of adhesion). In equilibrium the total energy  $U_m + U_s$  is minimal. Equilibrium can be determined by the detachment length  $l_0 - l_{x \text{ eq}}$  where  $l_{x \text{ eq}}$  is the distance from equilibrium. The critical length of microcantilevers is smaller than the detachment length  $l_0 - l_{x \text{ eq}}$  because before complete detachment shear deformation at the tip will occur and the beam will touch the substrate under an angle [16, 17].

The deformation energy at the point of snap back is about four times lower, and the critical length is [17, 18]:

$$l_{crit} = 4 \sqrt{\frac{3}{8} \cdot \frac{E \cdot t_0^3 \cdot g_0^2}{\gamma_s}} \quad (11)$$

### 3. EXPERIMENTAL INVESTIGATIONS

#### 3.1. Investigated microcantilever beams

The basic actuation designs are considered. These consist of suspended gold cantilevers with different geometrical dimensions, as shown in the insets of Fig. 4. The Young's modulus taken into consideration is  $E = 80 \text{ GPa}$ . The microstructures were made in 10 lithography and deposition steps using a wafer substrate of silicon, with a gap  $g_0$  between flexible part and substrate of about  $2 \mu\text{m}$  (Fig. 4). The dimensions of the flexible part are:  $l_0 = 190, 230, 280, 340, 410$  and  $490 \mu\text{m}$ ;  $w_0 = 35 \mu\text{m}$ ;  $t_0 = 2 \mu\text{m}$ . The beam anchor has a quadrate cross-section with a side of  $110 \mu\text{m}$  and a thickness of  $4 \mu\text{m}$ .

### 3.2. Experimental procedure

In order to determine the real value of Young's modulus needed in analytical and numerical computation, nanoindentation of the cantilever material directly on anchor was performed. The experimental values are interpreted using XEI software based on the Hertzian model.

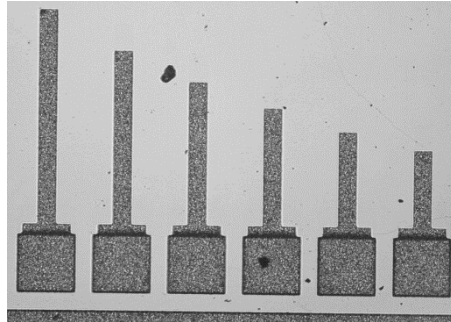


Fig. 4 – Cantilevers for experimental tests.

Figure 5 shows the indentation depth of gold material performed on the cantilever anchor using a four-side pyramid tip. In ambient condition the effective Young's modulus is 79.81GPa, a close value to the bulk Young's modulus of gold (80 GPa) [19].

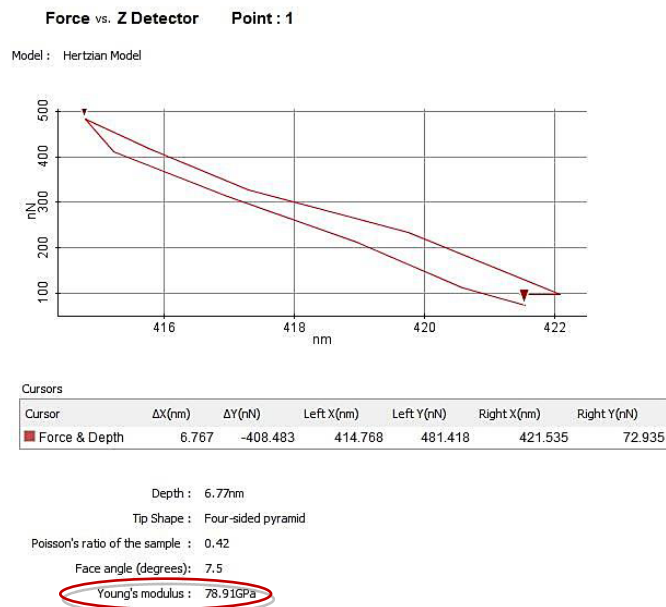


Fig. 5 – Nanoindentation test of microcantilever material.



### 3.2.1. Thermal expansion of a microcantilever

In order to determine the influence of temperature on thermal expansion measurements of a free-end microbeams above described we used an atomic force microscope (AFM-XE 70). The samples were maintained at a given temperature for 2–3 minutes before measurements. Measurements were performed at atmospheric pressure over a range of processing temperatures between 20°C and 100°C. A thermal controller stage was used to change and control the sample temperature. This device allows to keep the set temperature value during the measurements to an accuracy of 0.1°C.

The longitudinal thermal expansion of microcantilever depends on both the expansion of the flexible part and also the expansion of the anchor. If cantilever is used as a thermal actuator then it is only interested in change dilation of the free end beam. Consequently, with the AFM were monitored only thermal displacements in the  $x$  direction (Fig. 1).

Based on eq. (1) and considering the literature value for  $\alpha$  ( $\alpha = 14.2 \cdot 10^{-6} \text{ 1/}^\circ\text{C}$  for gold), we calculate a longitudinal thermal expansion for the cantilevers array. More exactly, at 100°C the thermal expansion is around 1.5 $\mu\text{m}$  for the shortest cantilever and 3.56 $\mu\text{m}$  for the longest cantilever.

### 3.2.2. Evaluation of the influence of temperature on bending stiffness

For experimental determination of the length influence on the cantilever stiffness, the above described samples with the length from 190  $\mu\text{m}$  to 490  $\mu\text{m}$  length were investigated. At the same time it was highlighted the influence of temperature on stiffness, changing the temperature within the range of 20–100 degrees.

Stiffness of investigated cantilevers is experimentally determined based on force versus deflection of the tested specimens. Investigations were performed with an acoustic isolated and environment controlled atomic force microscope (AFM) XE 70 using the contact mode. Each measurement was repeated many times in order to improve the accuracy of the experimental results. The cantilever used for investigation in contact mode is type HQ-NSC 35/Hard/Al BS with a nominal value of the spring constant  $k = 16 \text{ N/m}$  and radius  $< 20 \text{ nm}$ . In all experiments the bending force was applied to the free-end of the cantilever. The experimental data collected was imported into the XEI analysis software.

During AFM tests the vertical piezoelectric displacement of the scanning head  $z_{\text{piezo}}$  is controlled and the bending deflection of AFM probe is optically monitored. The bending deflection of cantilevers can be determined as  $z_{\text{sample}} = z_{\text{piezo}} - z_{\text{AFM}}$ . Slope of the load versus displacement experimental curve provides the stiffness of the microcantilevers.

The investigated cantilevers were also numerically analyzed with the Finite Element (FE) method using ANSYS Workbench 13.0 software. During tests a

thermal gradient is applied on cantilever and a mechanical force is used to bend it toward substrate. Using the same geometrical dimensions as in the experiments the samples were modelled and their response (out of plane deflection) for a given temperature and force was computed (Fig. 6).

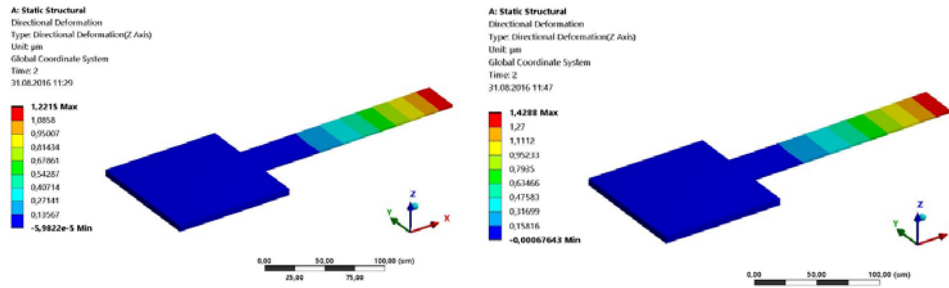


Fig. 6 – Finite element analysis of the axial expansion of 190µm microcantilever at 20°C and 100°C.

The simulations consist of two steps: first only the temperature was increased with no mechanical load; in the second step temperature was kept constant and a mechanical load was applied at the free end of the cantilever. Stiffness calculation took into account only the out of plane deflection due to mechanical force, thus from the total deflection was extracted that due to temperature increase.

A good correlation between the stiffness obtained based on numerical, analytical and experimental results at room temperature (20°C) are observed (Fig. 7).

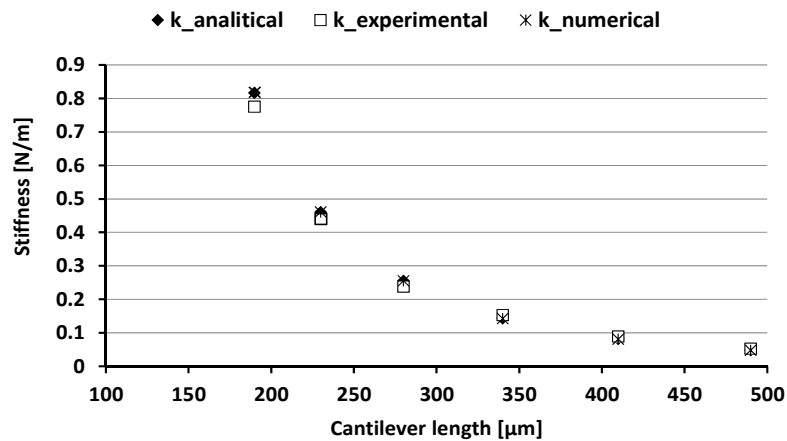


Fig. 7 – Analytical, numerical and experimental bending stiffness versus samples length at 20°C.

In the stiffness versus temperature variation chart (Fig. 8) it can be seen for all cantilevers a decrease in stiffness with increasing temperature. The percentage of experimental bending stiffness decrease with the temperature is around 22%

decrease for all microcantilevers. For instance, at 20°C for shortest cantilever the experimental stiffness is  $k = 0.7752$  N/m and at 100°C,  $k = 0.5878$  N/m. For the longest one at 20°C,  $k = 0.052$  N/m and at 100°C,  $k = 0.041$  N/m. It is obvious that the stiffness decreases with increasing the length of cantilever. The effect is due to the presence at higher temperatures of the thermal prestress considering that the anchor and the substrate are made of silicon that have a smaller thermal expansion coefficient than the cantilever of gold. The numerical analysis shows a smaller decrease in stiffness with the temperature ( $\sim 7\%$ ), for numerical analysis a constant Young's modulus has been considered instead of temperature dependent ones in reality.

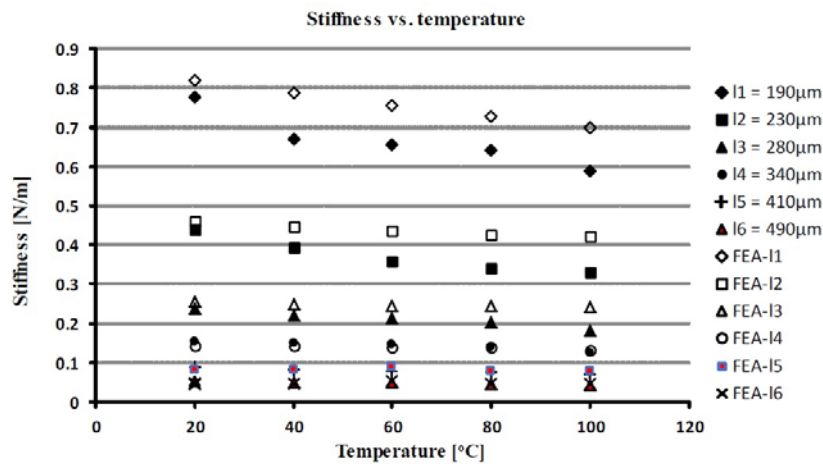


Fig. 8 – Experimental variation of the bending stiffness with temperature for investigated microcantilevers.

It mentions that the force that holds atoms together in atomic bonds decreases as these bonds grow in length, which happens during thermal expansion. This force is the origin of modulus of elasticity in macro scale. Therefore, at micro-nano scale, with increasing temperature modulus of elasticity undergoes a considerable decrease [10, 20, 21].

### 3.2.3. Adhesion evaluation

The adhesive effect between AFM probe ( $\text{Si}_3\text{N}_4$ ) and sample can be evaluated using the force spectroscopy mode of AFM so-called force/distance measurements, in a clean environment (clean room). This type of measurements allows deducing the force of adhesion between nanoscale rough surfaces of microcantilever. The AFM tip was brought in contact with the thin film surface and the adhesion force was measured from the pull-off point on the force distance curve. No additional loading force was applied during the point of contact.

This measurement provides correct information about surface energy and adhesion only if the contact between AFM tip and cantilever surface remains in the elastic range.

Literature indicates that at 20°C, there is no significant change in adhesion force when the load capacity is about 20 nN to 250 nN. Consequently, adhesion force measurements in this work were typically carried out in the low load regime when the contact is elastic and when no material transfer occurred at these loads. The adhesion force we measured here is mainly caused by the van der Waals and capillary interactions between a tip and the substrate.

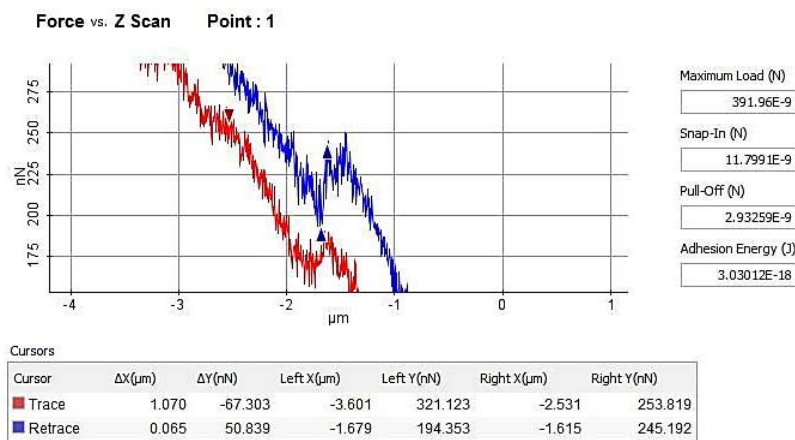


Fig. 9 – Adhesion force for cantilever with length  $l = 410\mu\text{m}$  at 40°C (zoom area).

In our experimental tests of adhesion forces, the microcantilevers are in contact with a  $\text{Si}_3\text{N}_4$  AFM tip HQ-SC 35/Hard/Al BS with a nominal value of the spring constant  $k = 16 \text{ N/m}$  and radius  $< 20 \text{ nm}$ . The load applied for all measurements was 50 nN. Measurements were performed over a range of processing temperatures between 20°C and 100°C and a contact time up to few seconds. All the experimental data collected was imported into the XEI analysis software. The pull-in and pull-off forces value are directly provided by the software (Fig. 9). For instance in Fig. 9 is presented the adhesion effect between the AFM tip ( $\text{Si}_3\text{N}_4$ ) and the investigated gold cantilever of length 410  $\mu\text{m}$  at 40°C.

The experimental variation of adhesive force between the AFM tip and the investigated gold microcantilevers as a function of temperature is summarized in Fig. 10. It was obtained experimentally a decrease of adhesion force with 20%–25% when the temperature increases to 100°C. Also we have obtained an increase in the adhesion while increasing the length of cantilevers. For example in sample 1 with a length of 190  $\mu\text{m}$  we obtained at the 20°C in environmental conditions (40%RH) an adhesion force of 14.3 nN and for a sample with a length of 490  $\mu\text{m}$  an adhesion force of 57.57 nN. Variability between the adhesion force measurements is expected,

as represented by the bars on each data point (5–10% percentage deviation between the 16 pull-off measurements).

Under ambient conditions, reducing the adhesion forces between the probe tip and microcantilever is limited by the existence of the meniscus force resulting from capillary condensation around the sites of contact between the tip and surface [22]. The capillary force between a tip and a substrate at the small nano-sized contacts of the surface asperities is due to the existence of a thin layer of water molecules adsorbed on the surfaces. The maximum capillary force is acting when the surfaces are in contact [22].

As we have already determined, the cantilevers investigated have a relatively small stiffness compared to the AFM tip. The tip would jump in contact with the substrate once the capillary force comes into play and stay in contact until break away during tip retractions.

However once the temperature increases the effect of wet thin layer on the cantilever surface will decrease leading to a lower adhesion force with increase of temperature (Fig. 10).

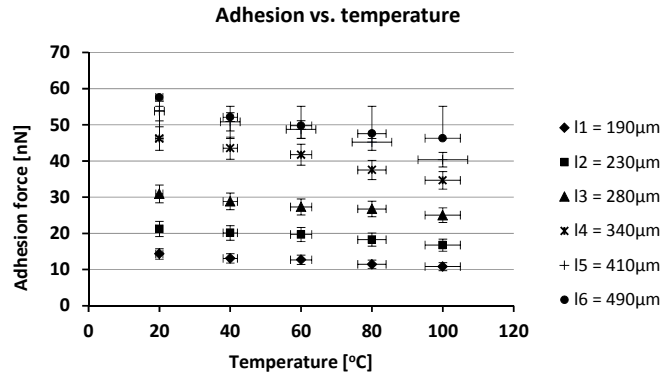


Fig. 10 – Experimental variation of the adhesion force with temperature for all investigated microcantilevers.

Two contact mechanic models derived by Johnson, Kendall, and Roberts theory (1971) and Derjaguin, Müller, and Toporov theory (1975), called the JKR and DMT models, respectively, are frequently used by researchers to interpret the pull-off forces measured by the AFM technique. The assumption of the theory is that the forces of attraction  $F$  at the contact area are identical to those outside of the area and give access to the thermodynamic work of adhesion [13, 23].

$$F_{(JKR)} = -\frac{3}{2} \cdot \pi \cdot \gamma_s \cdot R, \quad (12)$$

$$F_{(DMT)} = -2 \cdot \pi \cdot \gamma_s \cdot R, \quad (13)$$

where  $R$  is tip radius in nm (18 nm) and  $\gamma_s$  is the work of adhesion in  $\text{J}\cdot\text{m}^{-2}$ .

Based on two theories, DMT and JKR expressed by eqs. (13) and (14) and on the experimental values of the pull-off forces it was determined the work of adhesion. The results for the work of adhesion as a function of temperature for all microcantilevers in ambient environment are presented in Table 1.

Table 1

Work of adhesion based on the JKR and DMT theories

Sample	Temperature [ $^{\circ}\text{C}$ ] / Work of adhesion, $\gamma_{s\text{JKR}}$ and $\gamma_{s\text{DMT}}$ ( $\text{J}\cdot\text{m}^{-2}$ )									
	20 $^{\circ}\text{C}$		40 $^{\circ}\text{C}$		60 $^{\circ}\text{C}$		80 $^{\circ}\text{C}$		100 $^{\circ}\text{C}$	
	$\gamma_{s\text{JKR}}$	$\gamma_{s\text{DMT}}$	$\gamma_{s\text{JKR}}$	$\gamma_{s\text{DMT}}$	$\gamma_{s\text{JKR}}$	$\gamma_{s\text{DMT}}$	$\gamma_{s\text{JKR}}$	$\gamma_{s\text{DMT}}$	$\gamma_{s\text{JKR}}$	$\gamma_{s\text{DMT}}$
$l_1 = 190\mu\text{m}$	0.16	0.12	0.15	0.11	0.14	0.11	0.13	0.10	0.12	0.09
$l_2 = 230\mu\text{m}$	0.24	0.18	0.23	0.17	0.23	0.17	0.21	0.16	0.19	0.14
$l_3 = 280\mu\text{m}$	0.36	0.27	0.33	0.25	0.32	0.24	0.31	0.23	0.29	0.22
$l_4 = 340\mu\text{m}$	0.54	0.40	0.51	0.38	0.49	0.36	0.44	0.33	0.40	0.30
$l_5 = 410\mu\text{m}$	0.63	0.47	0.59	0.44	0.57	0.43	0.53	0.39	0.47	0.35
$l_6 = 490\mu\text{m}$	0.67	0.50	0.61	0.46	0.58	0.43	0.56	0.42	0.54	0.40

These results are consistent with results obtained in literature, namely in [18] for material couple  $\text{Si}_3\text{N}_4$  tip / Au using AFM technique an adhesion force of around 14 nN and work of adhesion  $148\text{ mJ}\cdot\text{m}^{-2}$  in ambient environment. The differences in adhesion data obtained with AFM is associated to differences in surface condition (surface preparation can vary from one laboratory to another), calibration technique used for cantilever stiffness and piezo, etc.

Based on these results and using Eq. 11 can be determined the critical length of microcantilevers which is smaller than the detachment length  $l_0 - l_{x\text{eq}}$  because before complete detachment shear deformation at the tip will occur and the beam will touch the substrate under an angle.

For instance, we obtained for the shortest microcantilever with length  $l_1 = 190\mu\text{m}$  the critical contact length of the beams that adhere to the substrate  $l_{\text{critic JKR}} = 8.69\mu\text{m}$  and  $l_{\text{critic DMT}} = 9.34\mu\text{m}$  at  $20^{\circ}\text{C}$ . At  $100^{\circ}\text{C}$ , the values are:  $l_{\text{critic JKR}} = 8.71\mu\text{m}$  and  $l_{\text{critic DMT}} = 9.36\mu\text{m}$ .

For the longest microcantilever with length  $l_1 = 490\mu\text{m}$  the  $l_{\text{critic JKR}} = 6.29\mu\text{m}$  and  $l_{\text{critic DMT}} = 6.77\mu\text{m}$  at  $20^{\circ}\text{C}$ . At  $100^{\circ}\text{C}$ , the values are:  $l_{\text{critic JKR}} = 6.25\mu\text{m}$  and  $l_{\text{critic DMT}} = 6.74\mu\text{m}$ .

In conclusion, for the shortest cantilever the critical length represents approximate 5% for total length of cantilever whereas for the longest one length represent approximate 1.3% for total length of cantilever, regardless the theory is working JKR or DMT. It is stated that for critical length calculation it was taken into account the relaxation modulus of elasticity with temperature based on Eq. 8.

#### 4. DISCUSSION AND CONCLUSIONS

Although microcantilevers are the most mature application of MEMS, they continue to improve and diversify. Microcantilevers area to use as microsensors is growing both in terms of technology as well as applications. Lately more players adhere to this area and more and more advanced devices are developing.

Although these sensors standardization remains a touchstone, there are groups of researchers contributing to the elimination of these obstacles. A good example of such progress is the new standard for smart sensors (i.e., IEEE 1451) [24].

Deformation of the materials due to thermal effects can be used to actuate devices, forcing the increase of temperature in the device. Knowledge of the influence of temperature on mechanical properties of nanostructures is essential for their use at the atomic scale which behaves qualitatively different at the nanoscale than at larger sizes.

Cost savings and increased performance microsensors, microactuators and microsystems will enable an unprecedented understanding and control of our physical world.

The cantilever sensor field is exciting and dynamic. The limit for detection is constantly challenged and only the imagination sets the limit to new applications [15]. Therefore the good understanding of the phenomena that occur to get a high-performance device is essential.

Because the adhesion force is calculated by multiplying the maximum vertical deflection of the cantilever with the cantilever stiffness, the precise knowledge of the cantilever stiffness is thereby essential to obtain reliable results. The stiffness vs. temperature variation for all samples presents a decrease in stiffness with increasing temperature. Set of cantilevers chosen for investigation whose length varies with a function of the third degree provide the same decrease in stiffness with temperature increase. The percentage of variation is around 22% decrease for all microcantilevers, due to the presence of the thermal prestress and decrease of the modulus of elasticity. At micro-nano scale, with increasing temperature the modulus of elasticity undergoes a significant decrease.

On the other hand a major challenge for MEMS designers is to overcome the effects of stiction and the source of stiction is the adhesion force. Therefore, adhesion is by far the most important parameter that must be minimized to improve the reliability of MEMS/NEMS operating in intermittent or continuous contact modes. Most often, a free-standing cantilever sticks to the substrate due to stiction in the final release step, situation that must be avoided. The adhesion force between AFM tip and cantilever acts as an additional force to the external force which is applied on the cantilever free end. This leads to increase the friction between surfaces so it is important to know its value.

In this work were followed two aspects: the experimentally evaluation of the adhesion force when the temperature increases from 20°C to 100°C when a decrease of adhesion force with 20%–25% was determined and then evaluation of the size effect of microcantilever on adhesion when we have obtained an increase in the adhesion with increasing the length of cantilevers. The contact length of the beams (the deflection length of the cantilever) that adhere to the substrate was determined starting from experimentally surface energy of the S-shaped beam.

Considering the experimental results presented in the paper concerning the adhesion effect, we can determine the value of adhesion force for the cantilever that interests us. The differences in experimental data obtained with AFM are associated to differences in surface condition (surface preparation can vary from one laboratory to another), calibration technique used for cantilever stiffness and piezo, etc.

In conclusion, the temperature dependence of the tribo-mechanical behavior of gold microcantilevers is of great importance in many applications of micro and nano engineering where accurate properties of the thermally actuated MEMS cantilevers are required within extended temperature range.

**Acknowledgments.** This work was supported by a grant of the Romanian National Authority for Scientific Research and Innovation, CNCS-UEFISCDI, project number PNCDI III - PED 33-2017.

*Received on July 18, 2017*

## REFERENCES

1. LOBONTIU, N., GARCIA, E., *Mechanics of microelectromechanical systems*, Springer Science & Business Media, 2004.
2. MALUF, N., WILLIAMS, K., *Introduction to microelectromechanical systems engineering*, Artech House, 2004.
3. VASHIST, S.K., *A review of microcantilevers for sensing applications*, J. of Nanotechnology, **3**, pp. 1–18, 2007.
4. ITOH, T., OHASHI, T., SUGA, T. *Piezoelectric cantilever array for multiprobe scanning force microscopy*, in: *An Investigation of Micro Structures, Sensors, Actuators, Machines and Systems*, IEEE Proceedings of The 9<sup>th</sup> Annual International Workshop on Micro Electro Mechanical Systems, San Diego, California, USA, February 11–15, 1996, pp. 451–455.
5. VOLDEN, T., ZIMMERMANN, M., LANGE, D., BRAND, O., BALTES, H., *Dynamics of CMOS-based thermally actuated cantilever arrays for force microscopy*, Sensors and Actuators A: Physical, **115**, 2, pp. 516–522, 2004.
6. KOMEILI, M., MENON, C., *Analysis and design of thermally actuated micro-cantilevers for high frequency vibrations using Finite Element Method*, World Journal of Mechanics, **6**, pp. 94–107, 2016.
7. FENG, Zhiping, ZHANG, Wenge, SU, Bindzki, Harsh, K.F., Gupta, K.C., Bright, V., Lee, Y.C., *Design and modeling of RF MEMS tunable capacitors using electro-thermal actuators*, IEEE MTT-S International Microwave Symposium Digest, Vol. 4, June 13–19, 1999, pp. 1507–1510.



8. RIETHMULLER, W. BENECKE, W., *Thermally excited silicon microactuators*, IEEE Transactions on Electron Devices, **35**, 6, pp. 758–763, 1988.
9. BARNES, J., STEPHENSON, R.J., WELLAND, M.E., GERBER, Ch., GIMZEWSKY, J.K., *Photothermal spectroscopy with femtojoule sensitivity using a micromechanical device*, Nature, **372**, 6501, p. 79–81, 1994.
10. LIFSHITZ, R., ROUKES, M.L., *Thermoelastic damping in micro-and nanomechanical systems*, Physical Review B, **61**, 8, pp. 5600–5609, 2000.
11. PUSTAN, M., ROCHUS, V., GOLINVAL, J.-C., *Mechanical and tribological characterization of a thermally actuated MEMS cantilever*, Microsystem Technologies, **18**, 3, pp. 247–256, 2012.
12. ZHAO, Y.-P., WANG, L., YU, T., *Mechanics of adhesion in MEMS – a review*, Journal of Adhesion Science and Technology, **17**, 4, pp. 519–546, 2003.
13. BIRLEANU, C., PUSTAN, M., *The effect of film thickness on the tribomechanical properties of the chrome-gold thin film*, IEEE – Symposium on Design, Test, Integration and Packaging of MEMS/MOEMS (DTIP), Budapest, Hungary, May 30 – June 2, 2016.
14. MARADUDIN, A.A., MAZUR, P., *Effects of surface roughness on the van der Waals force between macroscopic bodies*, Physical Review B, **22**, 4, pp. 1677–1686, 1980.
15. BOISEN, Anja, DOHN, Søren, KELLER, Stephan Sylvest, SCHMID, Silvan, TENJE, Maria, *Cantilever-like micromechanical sensors*, Reports on Progress in Physics, **74**, 3, p. 036101, 2011.
16. MASTRANGELO, C.H., HSU, C., *Mechanical stability and adhesion of microstructures under capillary forces. II. Experiments*, Journal of Microelectromechanical Systems, **2**, 1, pp. 44–55, 1993.
17. BHUSHAN, B., *Adhesion and stiction: mechanisms, measurement techniques, and methods for reduction*, Journal of Vacuum Science & Technology B, **21**, 6, pp. 2262–2296, 2003.
18. ACHANTA, S., CELIS, J.-P., *Nanotribology of mems/nems*, in: *Fundamentals of friction and wear on the nanoscale*, Springer, pp. 631–656, 2015.
19. PUSTAN, M., DUDESCU, C., BIRLEANU, C., *Nanomechanical and nanotribological characterization of a MEMS micromembrane supported by two folded hinges*, Analog Integrated Circuits and Signal Processing, **82**, 3, pp. 627–635, 2015.
20. TADAYON, M., SAYYAADI, H., JAZAR, G.N., *Nonlinear modeling and simulation of thermal effects in microcantilever resonators dynamic*, International MEMS Conference 2006, Singapore; Journal of Physics: Conference Series, **34**, 1, pp. 89–94, 2006.
21. PUSTAN, M., BIRLEANU, C., DUDESCU, C., BELCIN, O., *Temperature effect on tribological and mechanical properties of MEMS*, IEEE; 14<sup>th</sup> International Conference on Thermal, Mechanical and Multi-Physics Simulation and Experiments in Microelectronics and Microsystems (EuroSimE), Wroclaw, Poland, Apr. 14–17, 2013.
22. BUTT, H.-J., CAPPELLA, B., KAPPL, M., *Force measurements with the atomic force microscope: Technique, interpretation and applications*, Surface Science Reports, **59**, 1, pp. 1–152, 2005.
23. BHUSHAN, B., *Handbook of micro/nano tribology*, CRC Press, 1998.
24. JUDY, J.W., *Microelectromechanical systems (MEMS): fabrication, design and applications*, Smart Materials and Structures, **10**, 6, pp. 1115–1134, 2001.